Measurements in Harsh RF Propagation Environments to Support Performance Evaluation of Wireless Sensor Networks*

Kate A. Remley, Galen Koepke, Chris Holloway, Dennis Camell, Chriss Grosvenor
Electromagnetics Division, National Institute of Standards and Technology
Boulder, Colorado, 80305 USA
remley@boulder.nist.gov

Abstract: We describe methods for evaluating the performance of wireless devices such as wireless sensors in harsh radio environments. We describe how measurements of real-world propagation environments can be used to support the evaluation process. We then present representative measurement data from high-multipath environments where sensor networks are likely to be deployed: a fixed-infrastructure, process-control environment, here an oil refinery, and a heavy industrial environment, here an automotive assembly plant. The data are from an extensive set of studies carried out by the U.S. National Institute of Standards and Technology to provide open-literature data on radio-wave propagation over a wide frequency band in difficult radio-communication environments, including those with high loss and/or high multipath.

Keywords: Excess Path Loss; Modulated-Signal Measurement; Performance Evaluation; Performance Metric; Sensor Network; Wireless Communications

1. Background: Performance Evaluation of Wireless Sensors

To predict and verify the "over-the-air" operation of wireless devices, manufacturers and end users alike typically require a standardized method for evaluating the performance of the device. Often, the first step in this procedure involves developing an understanding of what signal impairments are likely to be encountered under standard operating conditions and how they will affect the transmitted signals. Performance metrics are then developed that can be used to evaluate the performance of the wireless device under the expected type and level of impairment. Here, we discuss the results of an extensive set of studies conducted in "harsh" radio propagation environments; that is, those where the transmitted signal experiences significant attenuation and/or multipath. We illustrate how data from these studies may be used for determining the type and level of signal impairments that wireless sensors may encounter in highly reflective environments.

Over-the-air performance evaluation of any wireless device is complicated by the fact that every environment presents a different set of features that may impact the device differently. Environmental factors that may impact wireless device behavior include both the physical environment (the geometry of features in the environment, the material from which they are made) and the electrical environment (other radio traffic, the presence of heavy machinery, and even the

* Publication of the U.S. government, not subject to copyright in the United States. This article appeared in Sensor Review, Vol. 29, no. 3, 2009, pp. 211 – 222. www.emeraldinsight.com/sr.htm.

movement of the radio within the environment). Evaluating a wireless device in one environment may not adequately represent its performance in another environment.

This problem can be overcome by using a standardized set of characteristics extracted from data measured in representative environments to design, test, and evaluate the performance of a device. Many segments of the wireless industry have identified a number of characteristics common to environments where their devices will be deployed, and from these, they have developed models of and test methods for representative environments. Most devices are designed to perform to a specified level of service within a given type of environment. Wireless device operation is then verified, before the device is released for sale, in a test bed whose physical characteristics mimic the representative environment. These same fundamental procedures are often used to evaluate wireless devices for other applications. A key aspect of this procedure is the extraction of significant electrical features from measurement data to allow classification and designation of representative environments.

There are some key differences between the required performance of many commonly used wireless devices, such as cellular telephones (cell phones) and wireless local area networks (WLANs), and wireless sensor networks. As a result, the use of existing wireless device performance specifications is not entirely sufficient for wireless sensor applications. One key difference between these applications is the need for a high level of reliability in many sensor applications. For applications such as cellular telephone communications, the user may be inconvenienced if the transaction is interrupted, but the session can be reconnected with little more than time lost. In sensor applications, such as those used for industrial process-control monitoring, situational awareness, physical security, or health care, increased operational costs and/or lives may depend on the reliability of the wireless sensor device or network. This means a higher standard for reliability of service must be maintained.

A second difference between some wireless applications and wireless sensor applications is that the latter typically involve radio communications where the sensors are physically nearer to each other than, for example, a cellular base station is to a cell phone. Many sensor networks use an ad-hoc networking model more similar to a WLAN, where the controlling node is relatively close to the sensor nodes. Sensor networks, like most WLANs, are usually lower-power applications, often limited to milliwatts of transmitted power by the use of Industrial, Scientific, and Medical (ISM) unlicensed frequency bands. Also, a cellular base station is usually physically located much higher than the controlling node in a WLAN or sensor network scenario. Unlike WLAN applications, in some sensor applications, the sensor nodes and the controller itself are both located relatively near to the ground, (a height of one meter or less). This physical difference in networks means that appropriate performance metrics must be developed.

A third difference between many common wireless device applications and wireless sensor networks is the size of the market. Vast resources have been spent on the multi-billion dollar cellular- and WLAN-communication

industries. The wireless sensor market share is a small fraction of that. As well, the use of wireless sensor technology is a relatively new field. As a result, few standards exist for specifying the performance of wireless devices or wireless sensors in many environments.

A final difference between many common commercial wireless applications and wireless sensor applications is that many common wireless devices have been designed for use in a set of radio environments different from those that may be encountered by sensor networks. For example, cellular telephones are typically designed to operate in outdoor environments, where long delay spreads may result in multipath that can cause intersymbol interference. WLANs were designed to operate in home or office environments, where the period needed for reflections to die out is limited, because the office or home space is relatively small and the construction materials are typically lossy. Wireless sensor networks are often designed to operate reliably within a wide range of environments, including large building structures, highly reflective industrial environments, and subterranean tunnels, to name but a few. These environments are often more challenging in terms of both path loss and the amount of both self interference (multipath) and interference from external sources. Fewer channel models exist for many of these environments as compared to the well-standardized commercial sector. In particular, there is a lack of open-literature data on radio-signal characteristics in harsh radio environments where point-to-point communications are used. Such data are necessary in order to develop channel models and laboratory-based test and verification methods.

Over the last several years, the U.S. National Institute of Standards and Technology has conducted measurements of various signal parameters in several harsh radio-propagation environments. We have found that the lack of impartial, rigorously collected data in these environments has hampered the development of both performance evaluation techniques and standards for a number of emerging wireless applications for the public-safety sector and industrial manufacturing community. Both of these communities are interested in taking advantage of the increased level of efficiency and ergonomics that wireless technology can offer. Applications such as inventory monitoring and environmental control, real-time video transfer, and robotics, as well as improved voice communications, are a few of the wireless applications being considered. However, few standards exist and even fewer sets of measurement data have been collected that address the special requirements of these sectors, which in many ways overlap with the special requirements of the wireless sensor community.

Our work has been funded by the U.S. Department of Justice through the Community Oriented Policing Services (COPS) Program and the NIST Office of Law Enforcement Standards (OLES), and USCAR, a collaborative effort between NIST and U.S. automakers. The intent of this work has been to provide real-world measurement data to aid in the development of technically sound performance metrics and standards. We present below representative examples

of our measurement results that may be particularly relevant to the wireless sensor community. The complete sets of data may be found in [1-6].

In this paper, we focus on measurements of parameters relevant to successful transmission of modulated signals including wideband channel frequency response, excess path loss, and root-mean-square (RMS) delay spread. We conducted tests in environments that are notoriously difficult in terms of multipath impairments to radio reception for emergency responders, but equally difficult for wireless sensor networks. The focus of the work presented here is on the characterization of the multipath environment, rather than other signal impairments such as weak-signal conditions or the effects of weather. However, it should be noted that both of these may also significantly alter the range of low-power wireless devices such as wireless sensors.

We present a selection of typical results from our studies, including an oil refinery and a factory-floor environment. We summarize measurement results from NIST Technical Notes 1546 [1] and 1552 [2] on the characterization of multipath in the propagation channel and discuss key findings that may be used to assess the performance of wireless devices such as sensors.

Occasionally product names are specified, solely for completeness of description, but such identification constitutes no endorsement by the National Institute of Standards and Technology. Other products may work as well or better.

2. Measurement of Wideband Channel Characteristics

In the studies of [1] and [2], we collected three types of data. The first type of data consisted of single-frequency received-power measurements collected continuously while walking through a structure. These data provide statistical information on the variability of signal levels throughout a structure. The second type of data was collected over a very broad frequency band at fixed points in the propagation environment. From the wideband data, we determined the excess path loss; that is, the attenuation or gain in excess of free-space path loss. After transforming the wideband data to the time domain, we calculated the root-mean-square (RMS) time-delay spread. The RMS delay spread is a figure of merit that quantifies the time it takes for signal reflections to die out in a given environment. We also collected modulated-signal measurements associated with broadband digitally modulated signals at 2.4 GHz and 4.95 GHz, the latter being allocated by the U.S. Federal Communications Commission (FCC) to the public-safety community. From these data, we found the error vector magnitude (EVM) in each environment. EVM is a figure of merit that describes the level of distortion in received, demodulated symbols of a digitally modulated signal. The complete data sets can be found in [1 – 6].

We present below examples of the wideband data, which can be used to study channel effects of either narrowband or wideband modulated signals. We give two examples of measurements in highly reflective environments where sensor networks may be deployed. These are an automobile manufacturing plant and an oil refinery. Again, our goal in collecting these data sets is to support the development of technically sound standards and performance evaluation

techniques for the public-safety and industrial communities, but these goals apply equally well to the wireless sensors community.

2.1 Measurement Set-up

We measured the wideband frequency response and time-domain parameters of the propagation environment using a measurement system based on a vector network analyzer (VNA), shown in Figure 1. This instrument can collect data over a very wide frequency range, from 25 MHz to 18 GHz for the system we used. Because a wideband transmitted signal corresponds to a short-duration pulse in the time domain, this system lets us measure the effects of the propagation environment on a narrow “synthetic” pulse as it travels from the transmitter to the receiver, including frequency-dependent losses and multipath reflections.

In the synthetic-pulse system, the VNA acts as both transmitter and receiver. The transmitting section of the VNA sweeps over a wide range of frequencies, a single frequency at a time. The transmitted signal is amplified and fed to a transmitting antenna.

The received signal is picked up over the air by the receiving antenna and sent back to the VNA via a fiber-optic cable. Transmitting the received signal along the fiber-optic cable maintains the phase relationships between the input and output signals, enabling reconstruction of the time-domain waveform associated with the received signal in post-processing. One advantage of this system is that it provides a high dynamic range relative to true time-domain-based measurement instruments. A disadvantage is the time it takes (several seconds) to collect the data, during which the channel may change in a dynamic environment.

In Figure 1, the system is configured for a line-of-sight reference measurement. In practice, the transmitting and receiving antennas may be separated by significant distances, although they must remain tethered together by the fiber-optic link. While directional horn antennas are shown in Figure 1, omnidirectional antennas were also used in our measurements. Omnidirectional antennas are most often used in sensor network applications. However, we can learn much about the characteristics of an environment using directional antennas that maximize gain in a specific direction and minimize the reception of multipath, as will be shown below.

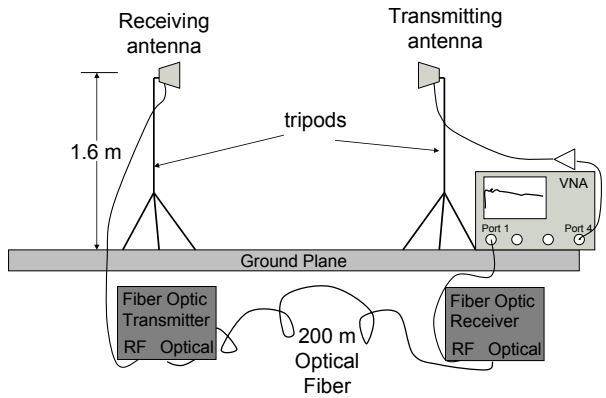

Figure 1: Synthetic-pulse measurement system based on a vector network analyzer. Frequency-domain measurements, synchronized by the optical fiber link, are transformed to the time domain in post-processing. This enables determination of excess path loss, time-delay spread, and other figures of merit important in characterizing broadband modulated-signal transmissions.

To make a measurement, the vector network analyzer is first calibrated by use of standard techniques where known impedance standards are measured. Then a reference free-space measurement is conducted, where the transmitting and receiving antennas are placed close enough together that environmental effects are negligible (although the received signal is gated to remove any environmental effects that are present). This reference measurement allows us to ratio out the response of the fiber-optic system, amplifiers, and any other electronics used in the measurement. The frequency response of the antennas is measured separately in the laboratory environment at NIST and is deconvolved in a post-processing step. We also high-pass filter our measurements in post-processing to suppress a large, low-frequency oscillation that occurs in the optical fiber link. The system is described in more detail in [1].

2.2 Excess Path Loss

Using the VNA-based system, we measured excess path loss over a wide frequency band at selected locations within each structure. Excess path loss (*EPL*) is typically defined as the loss or gain in excess of the loss that would be measured in a free-space environment [7, 8]:

$$EPL(f)_{dB} = TPL(f)_{dB} - FSPL(f)_{dB} \,. \tag{1}$$

In (1), *TPL* stands for the total path loss, the quantity that we actually measure in an environment, and *FSPL* stands for the free-space path loss. All three terms in (1) are typically functions of frequency. In a high-multipath or non-line-of-sight condition, the free-space path loss often cannot be measured directly. However, we can estimate the free-space path loss using a $1/R^2$

dependence in the received power level, where *R* is the spacing between the transmit and receive antennas, in meters.

As mentioned above, in order to calibrate out the nonidealities of our measurement system (cables, connectors, antenna effects, etc.), we first take a reference measurement at a specified distance between transmit and receive antennas. We then define the excess path loss as the difference between the reference measurement and total measured path loss, as follows:

$$EPL(f)_{dB} = TPL(f)_{dB} - 10\log\left(\frac{R_{\text{location}}}{R_{\text{reference}}}\right)^2 . \tag{2}$$

Note that we use the phrase "excess path loss" in the context of the vector-network-analyzer-based measurements, even though our graphs contain plots of normalized received signal power, not path loss. Graphs of path loss would have positive ordinates and increase with distance. However, the phrase "excess path loss" is traditionally used in the measurement community and will be used throughout this work.

2.3 RMS Delay Spread

The time-domain representation of the signal was calculated from the excess path loss data in post-processing. From this, we found the RMS delay spread, a figure of merit that gives an indication of the level of multipath interference encountered by the signal during transmission. RMS delay spread is calculated from the power-delay profile of a measured signal [9-11]. Figure 2 shows the power-delay profile for a representative building propagation measurement. The peak level usually occurs when the signal first arrives at the receiving antenna, although in high multipath environments we sometimes see the signal build up over time to a peak value and then fall off.

A common rule of thumb is to calculate the RMS delay spread from signals at least 10 dB above the noise floor of the measurement [11]. For the measurements described in the following sections, we defined the maximum dynamic range to be approximately 40 dB below the peak value. We chose 40 dB because signal levels below this contribute little to the calculated RMS delay spread, although this value was reduced for lower signal levels. For the illustrative measurement shown in Figure 3, we extended the window down to 70 dB below the peak value. Whether we use a 40 dB or a 70 dB threshold, the RMS delay spread does not change appreciably due to the almost constant slope of the power decay curve.

The RMS delay spread σ_τ can be defined as

$$\sigma_\tau = \sqrt{\overline{\tau^2} - \left(\overline{\tau}\right)^2} . \tag{3}$$

In (3), $\bar{\tau}$ is defined as the average value of the power-delay profile in the defined dynamic range window and $\overline{\tau^2}$ is the variance of the power-delay profile within this window.

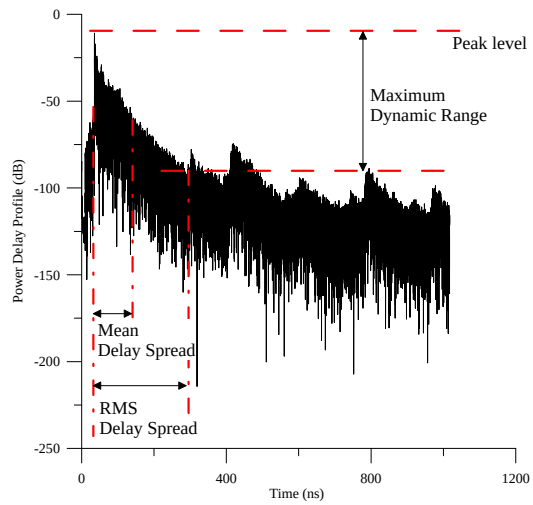

Figure 2: Power-delay profile for a building propagation measurement. The important parameters for a measured propagation signal are the peak level, the maximum dynamic range, the mean delay spread, and the RMS delay.

For the measurements reported here, the VNA-based measurement system was set up with the following parameters: the initial output power was set at −15 dBm to −13 dBm. The gain of the amplifier and the optical link and the system losses resulted in a received power level no more than 0 dBm. An intermediate-frequency (IF) averaging bandwidth of around 1 kHz was used to average the received signal. We typically recorded 6401 points per frequency band and chose the number of bands recorded in each measurement to avoid aliasing of the signal. We report here on both high-band and low-band measurements. Our high-band measurements range from 750 MHz to 18 GHz and were taken by measuring 48003 points in a total of three bands. Low-frequency band measurements, using one measurement band from 25 MHz to 1.2 GHz, are reported as well. The dwell time was approximately 25 μs per point.

3. Representative Results

The use of sensors in heavy industrial applications such as manufacturing and process control (refineries, utilities, etc.) is expected to increase in the future. Below, we describe representative wideband measurement data that were collected in two such highly reflective environments: an oil refinery and an automobile assembly plant. An understanding of the type and amount of multipath and attenuation in these propagation environments can help sensor device manufacturers to develop appropriate performance evaluation techniques.

3.1. Oil Refinery

Tests were carried out at an oil refinery near Denver, Colorado in March, 2007. The Suncor oil refinery is an outdoor facility covering many hectares with several intricate multi-story metallic piping systems, as shown in Figure 3(a). The piping complex is several hundred meters long. The tower in Figure 3(a) is nine stories high. In certain areas, the dense overhead piping forms a tunnel-like structure, such as the one shown in Figure 3(b), that can impede radio communications. Wideband excess path loss measurements are described here. Additional tests are described in [1, 12].

(a)

(b)

Figure 3: Oil refinery near Denver, Colorado. (a) Overview of the site. (b) Dense piping makes a tunnel-like propagation environment.

We carried out wideband measurements at 13 locations in the oil refinery in an area of very dense piping. Figure 4 shows the locations within the oil refinery where the measurements were made. The receive antenna, tethered to the VNA by the fiber-optic cable, was moved down the piping corridor shown in

Figure 3(b). We rolled the receive antenna along the path on a cart. The VNA was located in a test van made available for NIST use by the Institute for Telecommunication Sciences (ITS), a sister U.S. Department of Commerce organization at the Boulder Laboratories Site. A vertically polarized transmitting antenna was located on top of this van. For the low-frequency measurements, an omnidirectional transmit antenna was used, and for high-frequency measurements we used a directional horn antenna.

For locations 1-6, the vertically polarized receive antenna had a line-of-sight view of the transmit antenna. Once the receive antenna turned the corner, a non-line-of-sight condition existed.

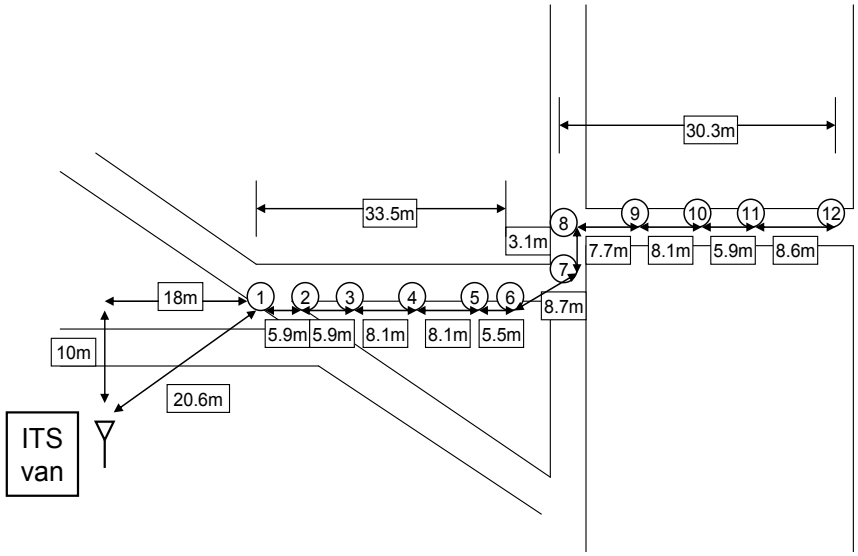

Figure 4: Layout of the test locations for the excess path loss measurements in the oil refinery complex. The test points were located under dense overhead piping and metallic structures, in most cases several stories high.

Figure 5 shows the measured excess path loss for frequencies between 25 MHz and 1.2 GHz at position 2 (near the opening of the piping), position 6 (several meters within the piping), and position 13 (deep within the piping). In each graph, the top curve represents the received power level relative to the estimated free-space path loss, and the bottom curve represents the noise floor of the measurement system. These measurements were made with omnidirectional antennas.

Because measurements were made outdoors in an operational facility, we see increased signal levels at commonly used frequency bands such as the 400 MHz two-way radio band, the 800 MHz cell-phone band, and the 900 MHz ISM band. There is also a strong signal component at frequencies around 200 MHz, which may correspond to broadband machine noise caused, for example, when the motor brushes in heavy machinery cross the gaps in the commutator.

Note the effects of strong reflections even at the opening of the piping structure (Figure 5(a)), shown by the deep nulls and peaks in the spectrum. Figure 5(b) also shows the effects of wideband multipath, but shows an increase in attenuation at the lower frequencies. This almost linear decrease in the received power, when compared to free-space values is due to a lossy waveguide effect of the overhead piping structure. As discussed in many articles on propagation in tunnels [13-15], once a few wavelengths separate the transmitter and receiver, the tunnel acts as a waveguide that strongly attenuates signals below the waveguide's cutoff frequency. Because the walls of the tunnel are not perfectly conducting, signals do propagate above the cut-off frequency but they experience significant loss.

Figures 6(a) – 6(c) show the measured excess path loss for frequencies between 1 GHz and 18 GHz at positions 2, 6, and 13 along the same path. In this case, directional antennas were used. At position 2, shown in Figure 6(a), the spectrum corresponding to the lower frequencies is quite flat, unlike for the lower-frequency case. Once the receive antenna is within the piping corridor, the excess path loss shows structure with frequency in the form of nulls and peaks caused by strong reflections, as shown in Figure 6(b). Then, as the receive antenna turns the corner and proceeds even further down the piping corridor, the signal drops off rapidly and is almost in the noise at position 13, Figure 6(c). The higher-frequency bands show greater attenuation with distance than do the lower-frequency bands. The complete set of excess-path-loss data is given in [1].

The RMS delay spread calculated from the VNA measurements is summarized in Figure 6(d). The lower-frequency band is shown by the line with circles, and the higher-frequency band is shown by the line with triangles. The delay spread remains relatively constant for positions 1 through 7 and again for positions 8 through 12. Beyond position 12, the signal is so weak that meaningful RMS delay spread values cannot be obtained.

The delay spread averages around 40 ns for both frequency bands for positions 1 through 7. When the transmitting antenna moves around the corner to position 8, we see a significant increase in RMS delay spread to approximately 140 ns for the lower frequencies and to approximately 80 ns for the higher frequencies. At position 8, the path is completely non-line-of-sight. The lower RMS delay spread value at the higher frequencies may be due to the use of directional antennas in that frequency band. Or, the pipes that cause the multiple reflections may be better reflectors at lower frequencies.

Note that the signals at the higher frequencies were close to the noise floor when the transmitter and receiver were separated by a great distance. This may have an effect on the accuracy of the RMS delay spread calculation at these points. However, the curves presented in Figure 6(d) show the trends clearly.

The data shown here indicate that significant radio traffic exists in the open-air, yet highly reflective, oil refinery. Thus, any deployment of wireless sensors should be designed to be immune to external interference. When a non-line-of-sight condition exists between transmitter and receiver, a significant amount of attenuation can occur. Thus, repeaters or mesh networking may need to be employed. Also, sensors operating at frequencies lower than about

500 MHz may experience additional attenuation due to the waveguide-below-cut-off effect. Performance evaluation protocols for wireless sensors that would be deployed in this type of environment should capture some of these key features to ensure robust and reliable performance of the sensor network.

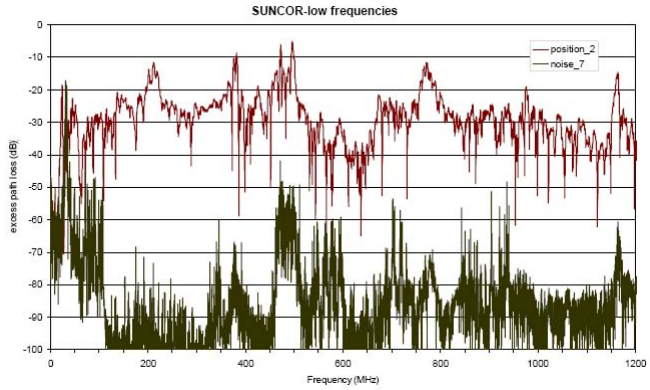

(a)

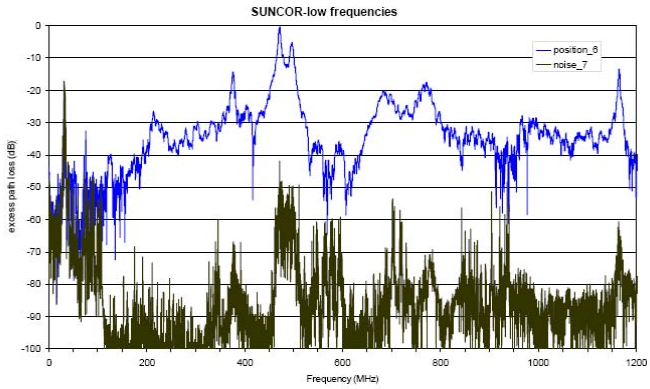

(b)

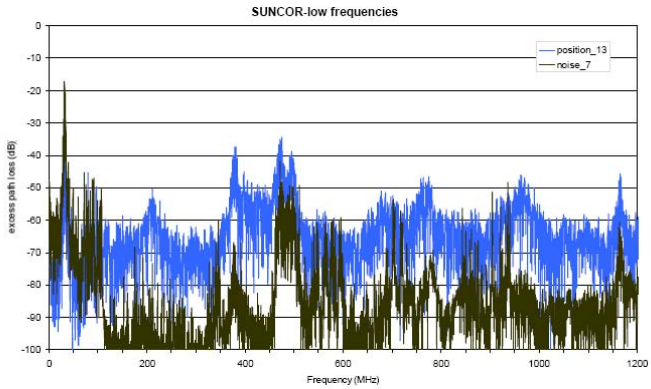

(c)

Figure 5: Excess-path-loss measurements at an oil refinery at (a) position 2, (b) position 6, and (c) position 13 for frequencies from 25 MHz to 1.2 GHz. The path was located outdoors but under dense piping several stories high.

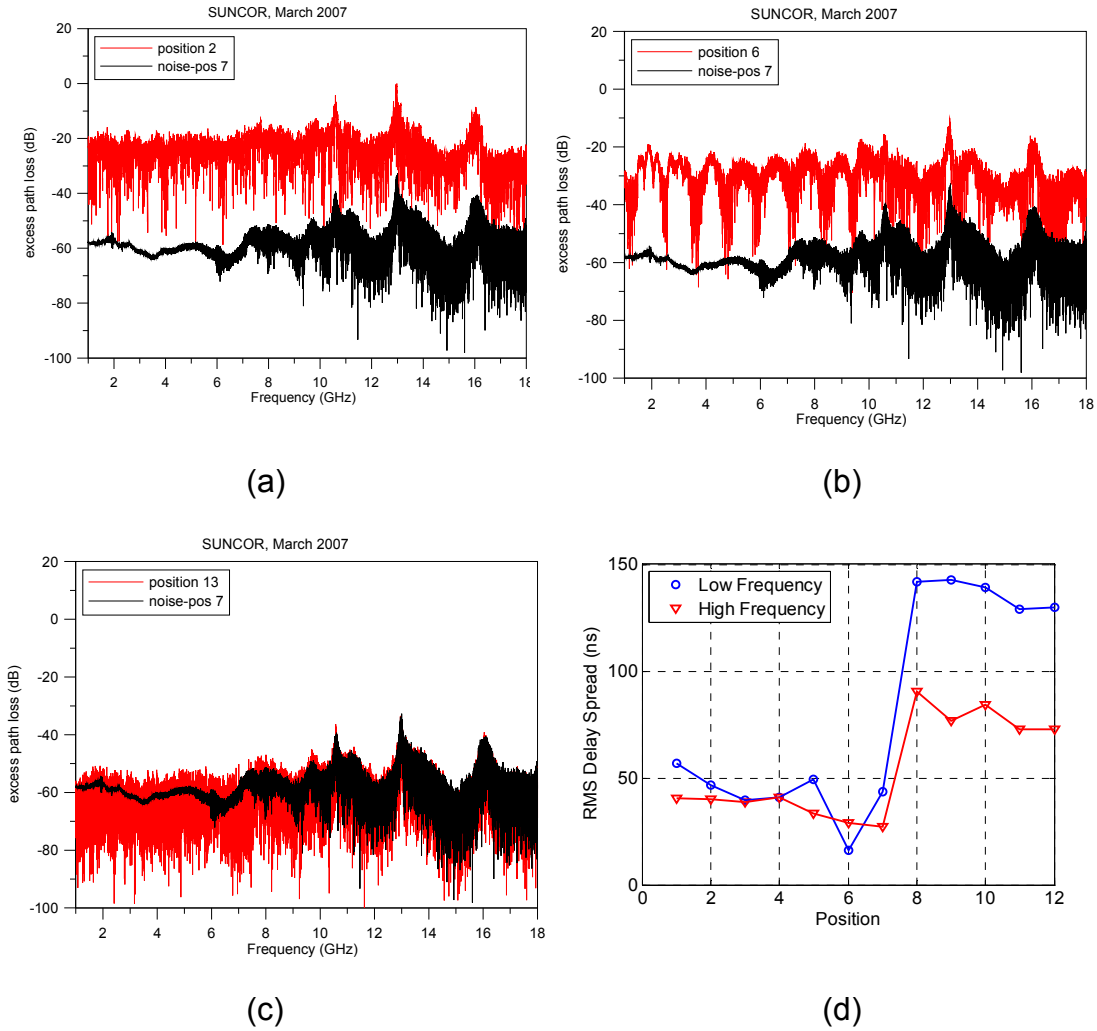

Figure 6: Excess-path-loss measurements at an oil refinery at (a) position 2, (b) position 6, and (c) position 13 for frequencies from 1 GHz to 18 GHz. The path was located outdoors but under dense piping several stories high. Attenuation was approximately 40 dB between 1 and 5 GHz when the receiver moved from position 2 to position 13, and was even greater at the higher frequencies. The RMS delay spread is shown in (d) for the positions shown in Figure 4 in the lower (circles) and higher (triangles) frequency bands.

3.2. Factory Floor: Automotive Assembly Plant

The second set of tests described here was conducted in an automotive assembly plant. As with the oil refinery, the industrial environment represented by this manufacturing plant contains metallic structures and objects that can have a significant effect on radio reception and affect the successful transmission of data from sensor networks. The size, shape, and materials of the factory environment, as well as the motion of the automotive chassis as they move down the assembly line, all play a role in successful wireless transfer of data from one sensor node to another.

The dimensions of the assembly plant were approximately 490 m x 230 m (1600 ft x 750 ft). The building was about 14 m (45 ft) high and constructed out of metal. The receiving site ("R" on Figure 7 below) was about 64 m (210 ft) from the left end of the building near column "S8". The column designators are noted on the left and upper side of the figure. For the excess path loss tests, a cart carrying the receive antenna moved down aisle "S" 300 m (approximately 985 ft) from the receiving location, along the path marked by the dashed line. Other tests, including measurements of the background ambient RF environment and measurements made in the 2.4 GHz ISM band, are reported in [2].

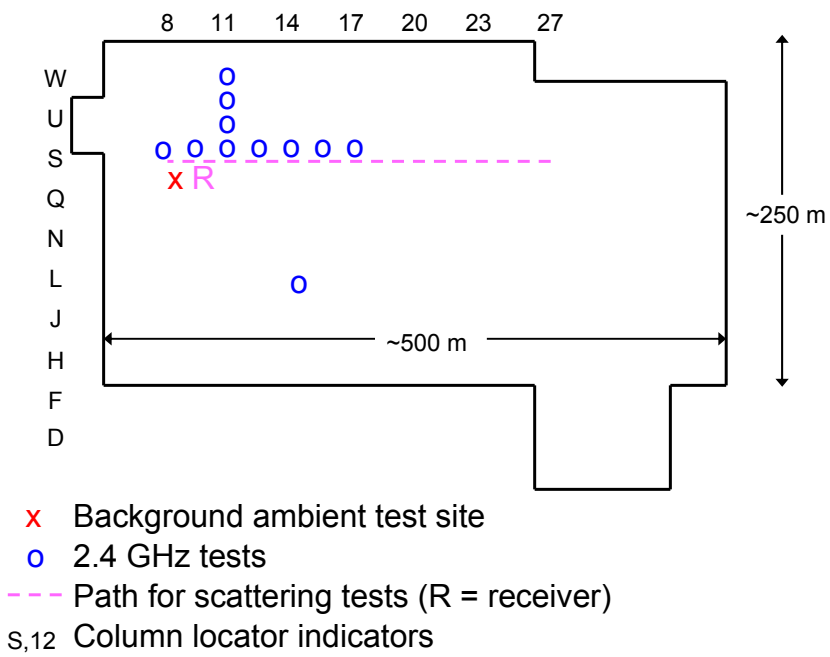

Figure 7: Rough outline of assembly plant where NIST wireless testing was carried out. The location of NIST receiving equipment is marked by an R. The dashed line indicates the path taken during the measurements of excess path loss.

For this series of tests, VNA measurement data were acquired at approximately 80,000 frequencies. For frequencies up to 1 GHz, omnidirectional antennas were again used. For frequencies from 1 GHz to 18 GHz, we used both directional dual-ridge waveguide antennas, similar to horn antennas, and

omnidirectional “top hat” antennas. The plant contained numerous assembly lines, catwalks, and other metallic objects and structures, as illustrated in Figure 8, where a diagram of the *in situ* measurement set-up is shown.

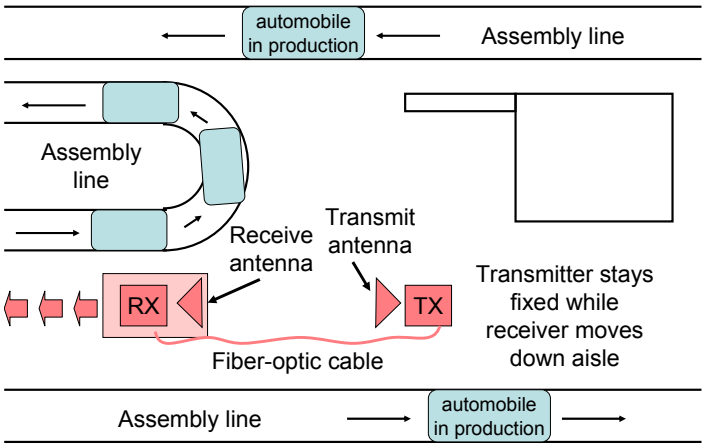

Figure 8: Layout of VNA tests in the assembly plant. The VNA (labeled “TX” for transmitter) remains in a fixed location. The signal received by the receive antenna (labeled “RX” for receiver) is amplified and returned to the VNA via the fiber-optic cable. The receiver was moved away from the transmitter along a straight line in discrete steps.

Figures 9(a) through 9(d) show measured excess path loss from the assembly plant over a frequency range from 100 MHz to 1.2 GHz. We show measurements taken for distances between the omnidirectional transmit and receive antennas of 20 m, 100 m, 150 m, and 250 m. Recall that the $1/R^2$ path loss has already been removed from these data, so the graphs show loss (or gain) due to additional attenuation in the plant as well as constructive and destructive interference due to multipath.

An overhead, open-framed second level of the plant was encountered approximately 80 m from the transmit antenna. Once the receive antenna moved under this metal-framed second level, Figures 9(b) – 9(d) again show the lossy waveguide effect described in the previous section on the oil refinery. The lower frequencies are significantly attenuated with respect to the higher frequencies, and the reduction in received power drops off almost linearly with frequency. For frequencies above approximately 800 MHz, the overall excess path loss decreases by only about 5 dB per 50 m. The rapidly changing multipath nulls and peaks seen as a function of frequency do not dip down to the noise floor of the receiver at the higher frequencies. This indicates that a sensor transmitting at frequencies above 800 MHz would have a better chance of being received than one transmitting at the lower frequencies.

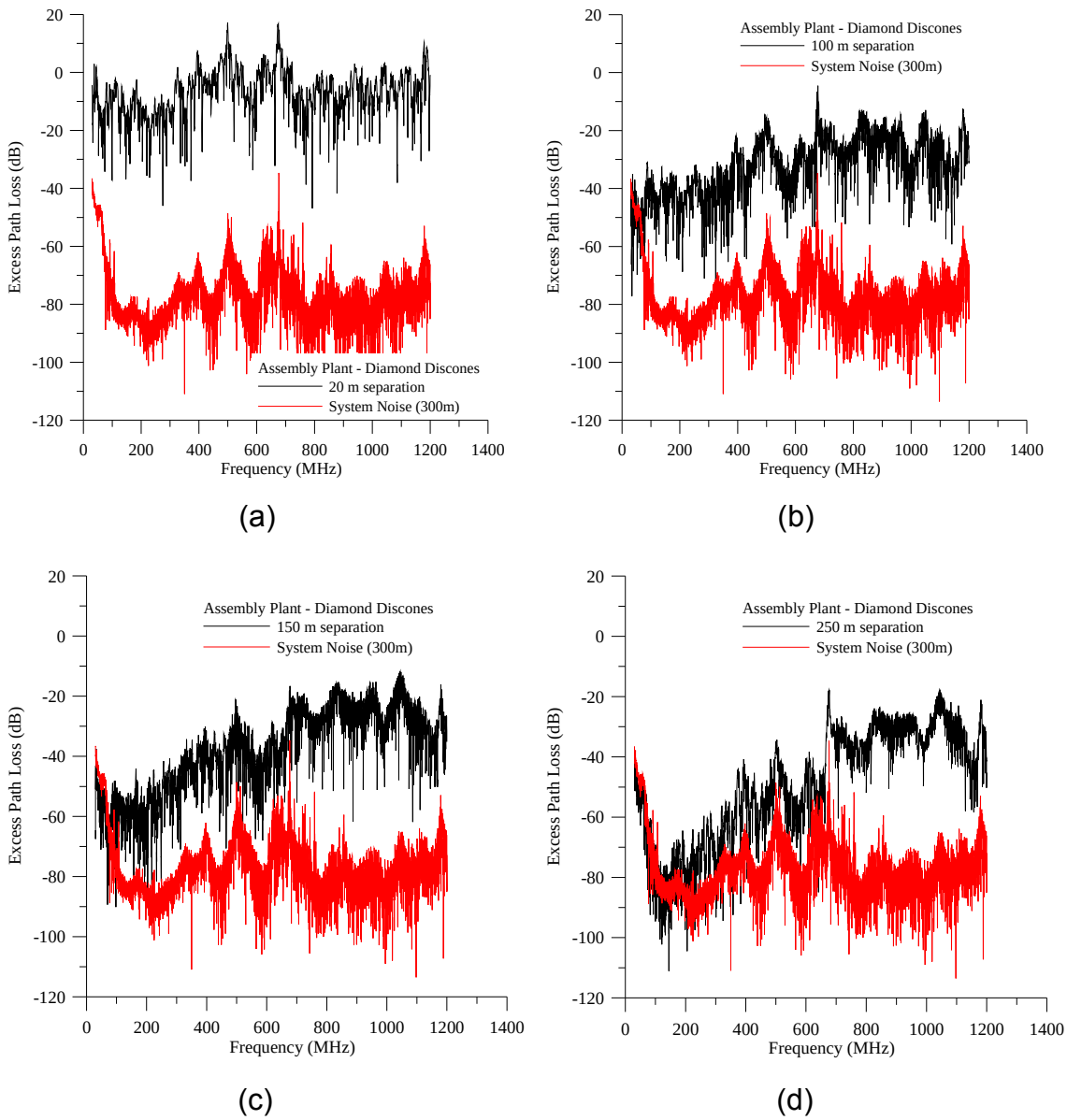

Figure 9: Excess path loss measured along a line-of-sight path from 100 MHz to 1.2 GHz in an automotive assembly plant. Separation distances between transmit and receive antennas are (a) 20 m, (b) 100 m, (c) 150 m, and (d) 250 m. Trade names are specified in the legend for informational purposes only and does not imply endorsement by NIST.

Figure 10 shows excess path data in the higher frequency band (1 GHz to 12 GHz) when a directional transmit antenna and an omnidirectional receive antenna were used. The rapid variation in the received power level indicates that multipath reflections are arriving from all directions around the receive antenna–both in a line of sight condition (directly down the aisle) and in a non-line-of-sight condition (reflected from objects throughout the plant).

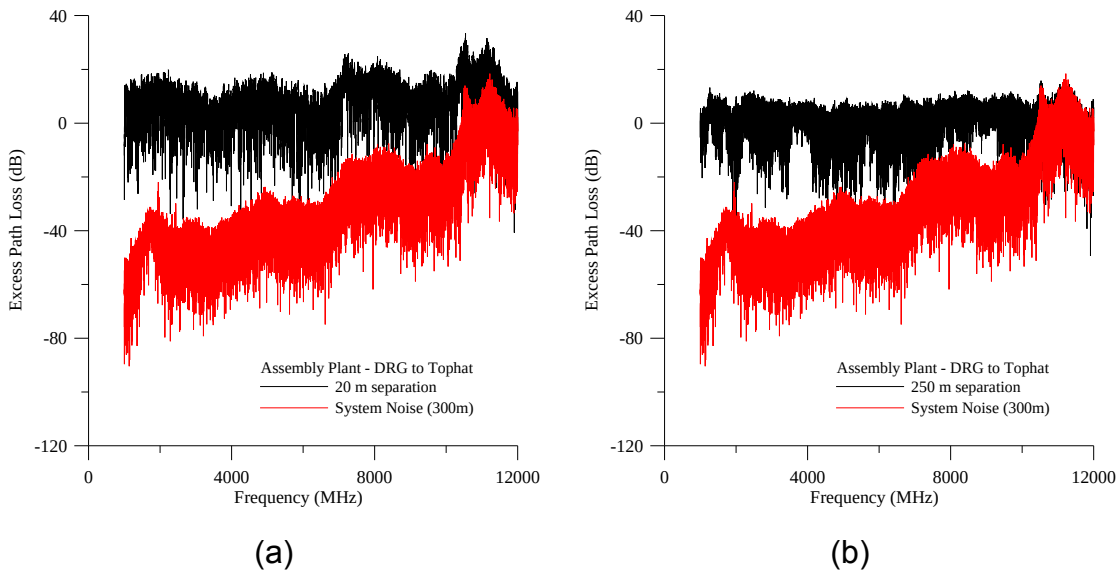

Figure 10: Excess path loss measured along a line-of-sight path from 1 GHz to 12 GHz in an assembly plant. The directional transmit and omnidirectional receive antennas were separated by (a) 20 m, (b) 250 m.

As in the oil refinery, we do not see the low-frequency roll-off due to the waveguide effect at these higher frequencies. We see that the overall level of the received power is not diminished significantly over that of free space, since the received levels are all around 0 dB. The increase over 0 dB is due to the gain of the directional antenna, which is around 10 dBi (a gain of ten decibels in the direction of propagation when compared to an isotropic radiator).

At 250 m for frequencies around 11 GHz and higher, the received signal level is attenuated such that it is at or below the noise floor of the measurement system. This is due in large part to the frequency response of the antennas that we used. A sensor device that is operated above 11 GHz may have difficulty transmitting at a sufficiently high level to be received if its dynamic range is comparable to that of the synthetic pulse system.

Figures 11(a) through 11(d) illustrate that the use of both transmit and receive directional antennas can reveal features in the propagation environment that may be masked when omnidirectional antennas are used. The effect of the directional antennas is to reduce the acquisition of multipath from directions other than that where the antenna is aimed. This allows study of the direct path in more detail. We plot the excess path loss at separation distances of 20 m, 100 m, 150 m, and 225 m.

Figure 11 also shows a deep notch in the excess path loss that increases in frequency the further the transmit and receive antennas are from each other. This is due to “ground bounce,” the reflection of the transmitted signal off the floor. Simple trigonometric formulas can be used to calculate the ground bounce if the height of the antennas is known. As the antennas are separated further, the angle of the ground bounce diminishes and the frequency where destructive interference between the direct and reflected signals occurs increases. At 250 m,

the notch was just above 12 GHz, so we show the result for 225 m here. Note that in a metal building, a ceiling bounce occurs as well, but in our case it occurred at a much lower frequency, due to the height of the ceiling. It could not be clearly distinguished in our measurements because of the obstructions in the ceiling path at separations greater than 80 m. This example illustrates that for fixed placement of wireless devices, including sensors, it is prudent to account for the most significant multipath effects, such as ground bounce, when the system is deployed.

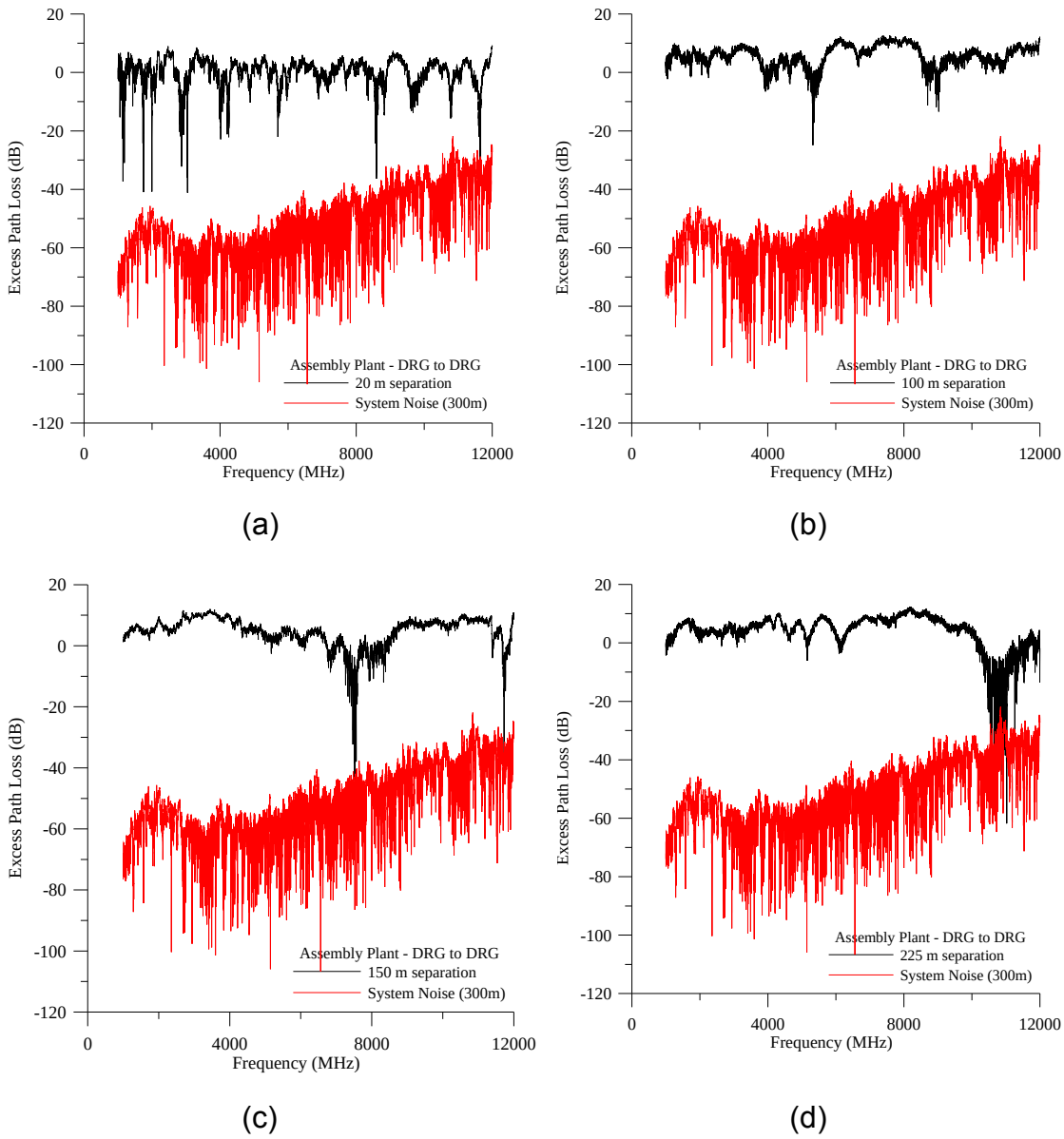

Figure 11: Excess path loss measured along a line-of-sight path from 1 GHz to 12 GHz in an assembly plant for various separation distances between transmitter and receiver. (a) 20 m, (b) 100 m, (c) 150 m, and (d) 225 m.

4.0 Conclusion

NIST has collected a large body of public-domain data on radio wave propagation in “difficult” propagation environments [1-6]. This work has focused on the measurement of parameters that are important for designing wireless systems that use digitally modulated signals, including attenuation, wideband excess path loss, and RMS delay spread. The measurement results presented here summarize some of the key effects found in [1-6] with respect to high-multipath environments where wireless sensor networks may be employed. The measurement techniques discussed above may be used to obtain measurements of the multipath environment over a wider frequency range that that of most commercially available systems. As a consequence, data such as these are rarely found in the open literature.

The excess path loss data from the highly reflective environments of the oil refinery and the automotive assembly plant show a number of key propagation features that are common to both environments. This includes multipath associated with line-of-sight propagation conditions, such as is found in Figures 6(b) and Figures 9 and 10. This type of multipath environment is characterized by a direct path signal plus a limited number of strong reflections. Graphs of excess path loss in this type of multipath environment typically show a structure with frequency, rather than fades that take on a random appearance with frequency.

Both environments studied here also exhibited waveguiding effects, where lower-frequency signals were attenuated relative to those at higher frequencies. Figures 5(b) and 9(c) and (d) illustrate this effect.

Multipath associated with non-line-of-sight propagation was seen in the oil refinery when the receive antenna turned a corner (Figures 5(c) and 6(c)), and when we used omnidirectional receive antennas in the automotive plant (Figure 10).

Use of data measured in real-world environments such as these is one of the first steps in developing rigorous, standardized performance evaluation methods for wireless devices, including wireless sensors. Understanding the type and level of signal impairments in representative environments enables the development of performance metrics that summarize device performance when subjected to a similar type of signal impairment. For example, most system designers can relate RMS delay spread to probable data loss for a given transmission format. The values of RMS delay spread for the line-of-sight case in the oil refinery (around 50 ns as shown in Figure 6(d)) may be sufficiently low for error correction schemes to prevent data loss. In the non-line-of-sight condition, the value of RMS delay spread doubles for the higher frequency measurements and almost triples for the lower frequency measurements. These may or may not cause problems, depending on the system.

The combination of performance metrics and measured data can, in turn, be used to develop models that help designers create devices that meet certain performance criteria. The measured data and performance metrics can also be used in the development of laboratory-based test beds, where hardware performance can be verified. The latter is a topic of current research at NIST [16].

Acknowledgements
This work was funded in part by the NIST Office of Law Enforcement Standards, Dereck Orr, Program Manager, and the NIST/United States Council for Automotive Research (USCAR) Collaboration, Dr. John Slotwinski, Liaison. The authors would like to acknowledge the contributions of members of the NIST Electromagnetics Division who assisted in data collection and processing, including John Ladbury, Robert T. Johnk (now with ITS), and Andrea Garuti.

5.0 References

[1] K.A. Remley, G. Koepke, C.L. Holloway, C. Grosvenor, D. Camell, J. Ladbury, D. Novotny, W.F. Young, G. Hough, M.D. McKinley, Y. Becquet, J. Korsnes, “Measurements to Support Broadband Modulated-Signal Radio Transmissions for the Public-Safety Sector,” *Natl. Inst. Stand. Technol. Note 1546*, Apr. 2008.

[2] K.A. Remley, G. Koepke, C. Grosvenor, R.T. Johnk, J. Ladbury, D. Camell, J. Coder, “NIST tests of the wireless environment in automobile manufacturing facilities,” *Natl. Inst. Stand. Technol. Note 1550*, Oct. 2008.

[3] C.L. Holloway, W.F. Young, G. Koepke, K.A. Remley, D. Camell, Y. Becquet, “Attenuation of Radio Wave Signals Coupled Into Twelve Large Building Structures,” *Natl. Inst. Stand. Technol. Note 1545*, Apr. 2008.

[4] C.L. Holloway, G. Koepke, D. Camell, K.A. Remley, S.A. Schima, M. McKinley, R.T. Johnk, "Propagation and Detection of Radio Signals Before, During, and After the Implosion of a Large Convention Center," *Natl. Inst. Stand. Technol. Note 1542*, June 2006.

[5] C.L. Holloway, G. Koepke, D. Camell, K.A. Remley, D.F. Williams, S.A. Schima, S. Canales, D.T. Tamura, "Propagation and Detection of Radio Signals Before, During, and After the Implosion of a Large Sports Stadium (Veterans’ Stadium in Philadelphia)," *Natl. Inst. Stand. Technol. Note 1541*, October 2005.

[6] C.L. Holloway, G. Koepke, D. Camell, K.A. Remley, D.F. Williams, S.A. Schima, S. Canales, D.T. Tamura, "Propagation and Detection of Radio Signals Before, During, and After the Implosion of a 13-Story Apartment Building," *Natl. Inst. Stand. Technol. Note 1540*, May 2005.

[7] B. Davis, C. Grosvenor, R.T. Johnk, D. Novotny, J. Baker-Jarvis, M. Janezic, “Complex permittivity of planar building materials measured with an ultra-wideband free-field antenna measurement system,” *Natl. Inst. Stand. Technol. J. Res.,* 112(1):67-73, Jan.-Feb., 2007.

[8] M. Riback, J. Medbo, J. Berg, F. Harryson, H. Asplund, “Carrier frequency effects on path loss,” *Proc. 63rd IEEE Vehic. Technol. Conf.*, Vol. 6, pp. 2717-2721, 2006.

[9] J.C.-I. Chuang, “The effects of time delay spread on portable radio communications channels with digital modulation,” *IEEE J. Selected Areas in Comm.*, SAC-5(5): 879-889, June 1987.

[10] Y. Oda, R. Tsuchihashi, K. Tsuenekawa, M. Hata, “Measured path loss and multipath propagation characteristics in UHF and microwave frequency bands for urban mobile communications,” *Proc. 53rd IEEE Vehic. Technol. Conf.*, Vol. 1, pp. 337-341, May 2001.

[11] J.A. Wepman, J.R. Hoffman, L.H. Loew, "Impulse Response Measurements in the 1850-1990 MHz Band in Large Outdoor Cells", *NTIA Report 94-309*, June 1994.

[12] K.A. Remley, G. Koepke, C.L. Holloway, C. Grosvenor, D.G. Camell, R.T. Johnk “Radio communications for emergency responders in high-multipath

outdoor environments," *Proc. 2008 Intl. Symp. Advanced Radio Tech.*, Boulder, CO, June 2008, pp. 106-111.

[13] A.G. Emslie, R.L. Lagace, and P.F. Strong, "Theory of the propagation of UHF radio waves in coal mine tunnels," *IEEE Trans. Antennas and Prop.*, vol. 23, no. 2, Mar. 1975, pp. 192-205.

[14] M. Rak and P. Pechac, "UHF propagation in caves and subterranean galleries," *IEEE Trans. Antennas and Prop.,* vol. 55, no. 4, April 2007, pp. 1134-1138.

[15] D. G. Dudley, M. Lienard, S.F. Mahmoud and P. Degauque, "Wireless propagation in tunnels," *IEEE Antennas Prop. Mag.,* vol. 49, no. 2, April 2007, pp. 11-26.

[16] E. Genender, C.L. Holloway, K.A. Remley, J. Ladbury, G. Koepke, H. Garbe, "Use of reverberation chamber to simulate the power delay profile of a wireless environment," *Proc. IEEE EMC Europe 2008*, Hamburg, Germany, Sept. 8-12, 2008.